Inhibition of Cullin-RING E3 ubiquitin ligase 7 by simian virus 40 large T antigen

Thomas Hartmann[a], Xinsong Xu[b], Mira Kronast[c], Susanne Muehlich[d], Kathleen Meyer[a,e], Wolfgang Zimmermann[c], Jerard Hurwitz[f,1], Zhen-Qiang Pan[b], Stefan Engelhardt[a,e], and Antonio Sarikas[a,e,1]

[a]Institute of Pharmacology and Toxicology, Technische Universität München, 80802 Munich, Germany; [b]Department of Oncological Sciences, Icahn Medical Institute, Mount Sinai School of Medicine, New York, NY 10029; [c]Tumor Immunology Laboratory, LIFE Center, Ludwig Maximilians University, 81377 Munich, Germany; [d]Walther Straub Institute of Pharmacology and Toxicology, Ludwig Maximilians University, 80336 Munich, Germany; [e]German Center for Cardiovascular Research, Partner Site Munich Heart Alliance, 80802 Munich, Germany; and [f]Program of Molecular Biology, Memorial Sloan-Kettering Cancer Center, New York, NY 10065

Contributed by Jerard Hurwitz, January 30, 2014 (sent for review July 26, 2013)

Simian virus 40 (SV40) large tumor antigen (LT) triggers oncogenic transformation by inhibition of key tumor suppressor proteins, including p53 and members of the retinoblastoma family. In addition, SV40 transformation requires binding of LT to Cullin 7 (CUL7), a core component of Cullin-RING E3 ubiquitin ligase 7 (CRL7). However, the pathomechanistic effects of LT–CUL7 interaction are mostly unknown. Here we report both in vitro and in vivo experimental evidence that SV40 LT suppresses the ubiquitin ligase function of CRL7. We show that SV40 LT, but not a CUL7 binding-deficient mutant ($LT^{\Delta 69-83}$), impaired 26S proteasome-dependent proteolysis of the CRL7 target protein insulin receptor substrate 1 (IRS1), a component of the insulin and insulin-like growth factor 1 signaling pathway. SV40 LT expression resulted in the accumulation and prolonged half-life of IRS1. In vitro, purified SV40 LT reduced CRL7-dependent IRS1 ubiquitination in a concentration-dependent manner. Expression of SV40 LT, or depletion of CUL7 by RNA interference, resulted in the enhanced activation of IRS1 downstream signaling pathways phosphatidylinositol-3-kinase/AKT and Erk mitogen-activated pathway kinase, as well as up-regulation of the downstream target gene *c-fos*. Finally, SV40 LT-positive carcinoma of carcinoembryonic antigen 424/SV40 LT transgenic mice displayed elevated IRS1 protein levels and activation of downstream signaling. Taken together, these data suggest that SV40 LT protects IRS1 from CRL7-mediated degradation, thereby sustaining high levels of promitogenic IRS1 downstream signaling pathways.

Studies with simian virus 40 (SV40), a member of the *Polyomaviridae* family of tumor viruses, have led to fundamental insights into molecular processes of cell transformation and oncogenesis (1, 2). SV40 encodes the large tumor antigen (LT) with the potential to transform cells in culture and induce tumors in rodents. The tumorigenic features of SV40 have been attributed to binding and deactivation of key tumor suppressor proteins of the host cell including p53 and members of the retinoblastoma (pRB) family (1–3). In addition, SV40 LT was shown to be physically associated with Cullin 7 (CUL7; also named p185 or p193) (4, 5) as well as insulin receptor substrate 1 (IRS1) (6). It has been proposed that the association of SV40 LT with either CUL7 or IRS1 is critical to SV40 oncogenic transformation (7–9). However, the functional effect of LT interaction with CUL7/IRS1 and their pathophysiological interrelation remains mostly unknown.

CUL7 is a scaffold protein responsible for assembling the multisubunit Cullin-RING E3 ubiquitin ligase 7 (CRL7) that consists of the RING-finger protein ROC1 and the Skp1-Fbw8 substrate-targeting subunit (10, 11). Genetic studies documented a pivotal growth-regulatory role of CRL7. Both *cul7* (12) and *fbw8* (13) null mice exhibit intrauterine growth retardation. In addition, *CUL7* germ-line mutations were linked to 3-M syndrome, a hereditary disorder characterized by pre- and postnatal growth retardation in humans (14, 15), as well as Yakut dwarfism syndrome (16). DeCaprio and colleagues mapped the CUL7 interaction domain on SV40 LT to residues 69–83 and demonstrated that the CUL7 binding-deficient deletion mutant ($LT^{\Delta 69-83}$) lost its transformation potential despite maintaining its ability to bind and inactivate p53 and pRB members (8, 9). This suggested that CUL7 may act as a tumor suppressor and that constraining growth-inhibitory functions of CRL7 may be critical to SV40 transformation.

We previously identified IRS1, a component of the insulin and insulin-like growth factor 1 (IGF1) signaling pathway, as a proteolytic target of CRL7 (17). Binding of insulin or IGF1 to its receptor induces tyrosine phosphorylation of IRS1 and subsequent activation of phosphatidylinositol-3-kinase (PI3K)/AKT and Erk mitogen-activated pathway kinase (MAPK) pathways (18). It was shown that CRL7-induced degradation of IRS1 is part of a negative feedback loop via mechanistic target of rapamycin complex 1 (mTORC1) to restrain IRS1 downstream signaling (17, 19). A more recent study suggested an mTORC2-dependent feedback inhibition of IRS1 by direct phosphorylation of Fbw8, resulting in enhanced stability of this F-box protein that promotes IRS1 degradation (20). Collectively, these studies have implicated roles for CRL7 in regulating both mTORC1 and mTORC2 signaling. Based on the above observations, we investigated whether SV40 LT impacts on CRL7 feedback regulation of IRS1 signaling in addition to its effects on p53 and pRB members.

Results

SV40 LT Impairs CRL7-Mediated Degradation of IRS1. We used a cell-based degradation assay to examine the effect of SV40 LT on the E3 ubiquitin ligase function of CRL7. V5-tagged IRS1 was

Significance

Simian virus 40 (SV40) large tumor antigen (LT) is a viral oncoprotein with the ability to induce tumors by inhibition of cellular tumor suppressors such as p53 and members of the retinoblastoma protein family. Here we present evidence for a role of SV40 LT in suppressing the activity of Cullin-RING E3 ubiquitin ligase 7 in mediating the ubiquitin-dependent degradation of insulin receptor substrate 1 (IRS1). This SV40 LT-mediated protection of IRS1 leads to enhanced activation of promitogenic downstream signaling pathways AKT and Erk mitogen-activated pathway kinase, which may contribute to viral-induced oncogenic transformation.

Author contributions: T.H., S.M., K.M., W.Z., J.H., Z.-Q.P., S.E., and A.S. designed research; T.H., X.X., M.K., S.M., K.M., Z.-Q.P., and A.S. performed research; T.H., X.X., M.K., K.M., W.Z., J.H., Z.-Q.P., and A.S. contributed new reagents/analytic tools; T.H., M.K., S.M., K.M., W.Z., J.H., Z.-Q.P., S.E., and A.S. analyzed data; and T.H. and A.S. wrote the paper.

The authors declare no conflict of interest.

[1]To whom correspondence may be addressed. E-mail: j-hurwitz@ski.mskcc.org or sarikas@ipt.med.tum.de.

This article contains supporting information online at www.pnas.org/lookup/suppl/doi:10.1073/pnas.1401556111/-/DCSupplemental.

BIOCHEMISTRY

expressed ectopically in HEK293 cells, and protein levels were monitored by immunoblot analyses. As expected, coexpression of the CRL7-specific F-box protein myc-Fbw8 resulted in a significant reduction of IRS1 protein level (Fig. 1 *A* and *B*, lane 2 vs. 3), which was prevented by treatment with the proteasomal inhibitor MG132 (Fig. 1 *A* and *B*, lane 3 vs. 4). Strikingly, coexpression of HA-tagged wild-type SV40 LT averted Fbw8-induced IRS1 degradation to a similar extent as MG132 treatment (Fig. 1 *A* and *B*, lane 5). In contrast, no significant effect on IRS1 steady-state level was observed after coexpression of the CUL7 binding-deficient mutant SV40 LT$^{\Delta 69–83}$ (Fig. 1 *A* and *B*, lane 6). Similar results were obtained in degradation assays with overexpression of CUL7 and Fbw8 (Fig. S1). Quantification of LT and LT$^{\Delta 69–83}$ by immunoblot analyses revealed no significant differences in expression levels (Fig. S2). Of note, transient expression levels of LT and LT$^{\Delta 69–83}$ were comparable to LT-transformed HEK293T or COS-7 cells (Fig. S3). To exclude the possibility that LT-mediated effects were due to changes in gene transcription, IRS1 mRNA was quantified by real-time PCR. No significant changes in IRS1 mRNA concentration were detected upon coexpression with either SV40 LT or LT$^{\Delta 69–83}$ (Fig. 1*C*). These findings indicate that SV40 LT interferes posttranscriptionally with the CRL7-mediated proteasomal degradation of IRS1.

To confirm and extend the above results, we measured the protein half-life of IRS1 in HEK293 cells and asked whether SV40 LT expression stabilizes the IRS1 protein. Cells were transfected with Fbw8, SV40 LT, or LT$^{\Delta 69–83}$ and cultured for 1 h in the presence of ^{35}S-labeled methionine and cysteine, followed by a chase with nonradioactive cell-culture medium. Labeled IRS1 protein was detected by autoradiography following V5 immunoprecipitation and SDS/PAGE. Immunoblot analysis of LT and LT$^{\Delta 69–83}$ in cell samples taken immediately before radioactive labeling revealed no significant differences in expression levels (Fig. S4). In keeping with previously published observations (17), the half-life of the IRS1 protein in the presence of ectopic Fbw8 was 4 h (Fig. 1*D*, white boxes). However, coexpression of SV40 LT markedly antagonized IRS1 decay and resulted in nearly constant IRS1 steady-state levels (Fig. 1*D*, black boxes). In contrast, the stability of the IRS1 protein was unaffected by the presence of the CUL7 binding-deficient mutant LT$^{\Delta 69–83}$ (Fig. 1*D*, black triangles). Collectively, these results are consistent with the hypothesis that SV40 LT binding to CUL7 interferes with the CRL7-mediated ubiquitination and proteasomal degradation of IRS1.

SV40 LT Impairs in Vitro Ubiquitination of IRS1 by CRL7. To evaluate whether SV40 LT directly interferes with CRL7 E3 ligase function, we reconstituted IRS1 ubiquitination by CRL7 in vitro using purified proteins. We recently reported that CRL7 mediates efficient ubiquitination of the N-terminal IRS1 fragment (residues 1–574) (19). GST-tagged IRS1$^{1–574}$ (designated GST-IRS1$^{1–574}$) was expressed using the baculovirus/insect cell system and affinity-purified. Ubiquitination was reconstituted by incubation of GST-IRS1$^{1–574}$ with CRL7, UbcH5c, E1, and ubiquitin, and the extent of ubiquitination was measured by anti-GST immunoblot analysis. As shown in Fig. 2, formation of high molecular weight species occurred, concomitant with a reduction of the input substrate by ∼70% (Fig. 2*A*, lane 3 vs. 2). Of note, increasing levels of SV40 LT resulted in higher amounts of unmodified GST-IRS1$^{1–574}$ (Fig. 2*A*, lanes 4–7 and Fig. 2*B*), indicative of reduced substrate ubiquitination. These data are consistent with the hypothesis that binding of SV40 LT to CUL7 stabilizes the IRS1 protein through impairment of CRL7 ubiquitin ligase function.

SV40 LT Interacts with the C Terminus of Cullin 7. To gain further insight into the potential mechanisms by which SV40 LT inhibits the action of CRL7, we next sought to map the SV40 LT-binding domain on CUL7. The 1,698-amino acid CUL7 protein contains several distinct motifs, such as the conserved cullin domain, the DOC domain (similar to DOC1 of the APC/C), and the CPH domain (conserved domain in CUL7, PARC, and HERC2 proteins) (21). For this purpose, HA-tagged deletion mutants of CUL7 spanning different domains of the protein (Fig. 3*A*) were coexpressed with V5-tagged SV40 LT in HEK293 cells and

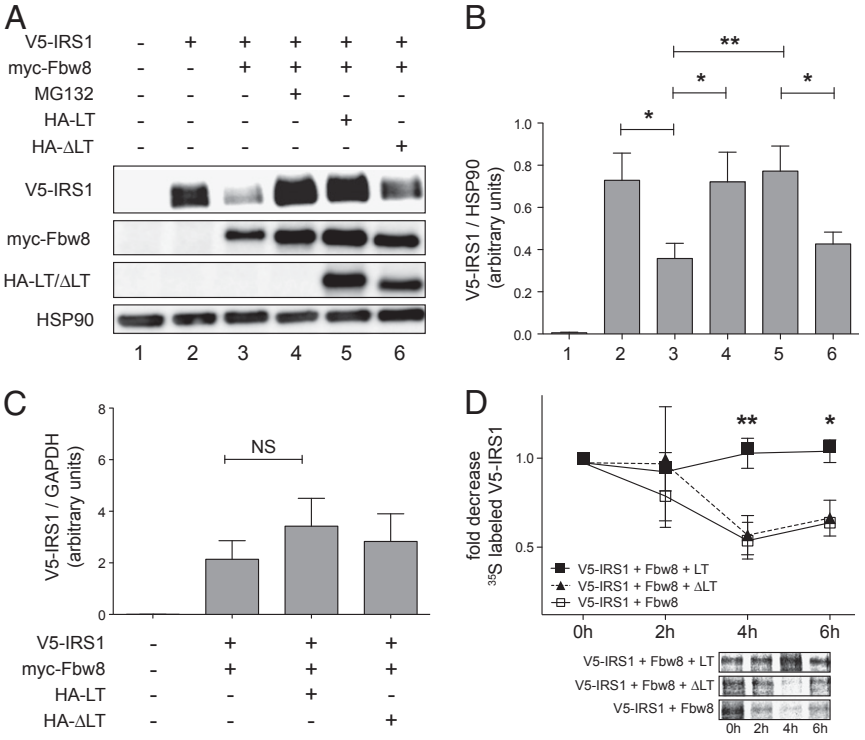

Fig. 1. CRL7-mediated degradation of IRS1 is impaired by SV40 LT. (*A*) HEK293 cells were transfected with empty vector or plasmids encoding V5-tagged IRS1, myc-tagged CRL7 substrate receptor Fbw8, HA-tagged LT, and HA-tagged CUL7 binding-deficient mutant LT$^{\Delta 69–83}$ (designated ΔLT). Where indicated, cells were treated with the proteasomal inhibitor MG132 (10 μM) for 8 h. Lysates were separated by SDS/PAGE and subjected to Western blot analysis. (*B*) IRS1 protein concentrations in HEK293 cells subjected to protein degradation assays as described in *A*. $n = 9$; $^*P < 0.05$, $^{**}P < 0.01$. (*C*) IRS1 mRNA concentrations in HEK293 cells subjected to protein degradation assays as described in *A*. The graph depicts quantitative real-time PCR data of five independent experiments. NS, not significant. (*D*) Stabilization of IRS1 steady-state protein level by SV40 LT. HEK293 cells were transfected with plasmids encoding V5-tagged IRS1, myc-tagged Fbw8, HA-tagged LT, and HA-tagged ΔLT. At 24 h after transfection, proteins were labeled for 1 h with [^{35}S]Met/Cys and chased with normal growth medium. Cell extracts were subjected to V5 IP, separated by SDS/PAGE, and visualized by autoradiography (*Lower*). $n = 4$; $^*P < 0.05$, $^{**}P < 0.01$. Data are presented as means ± SEM.

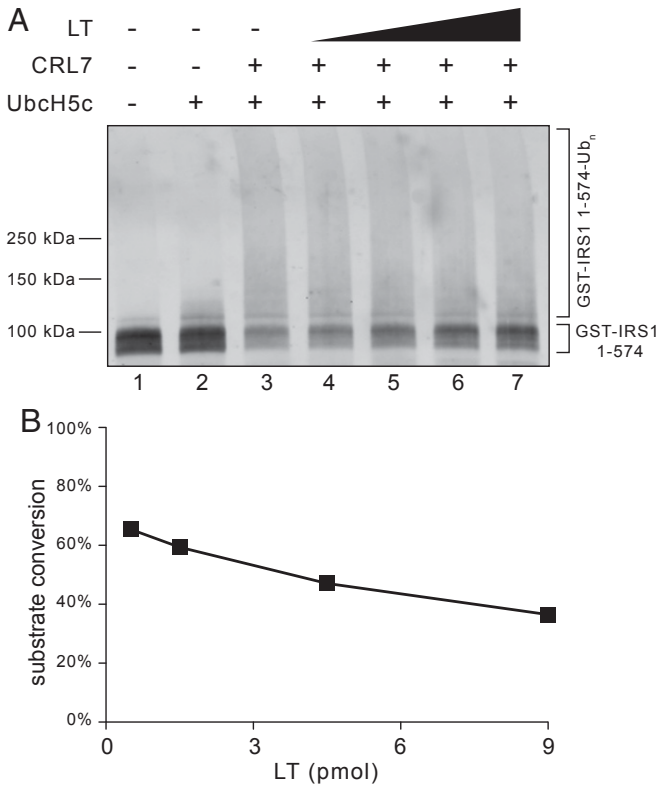

Fig. 2. Effect of SV40 LT on the ubiquitination of IRS1$^{1–574}$ by CRL7. (*A*) The in vitro ubiquitination reaction was reconstituted as described (19) and increasing amounts of purified SV40 LT (0.5, 1.5, 4.5, and 9 pmol) were added. (*B*) Quantification of input substrate levels after reaction revealed an inhibitory effect by SV40 LT.

coimmunoprecipitation experiments were performed. Full-length CUL7 and the CUL7 binding-deficient mutant LT$^{\Delta 69–83}$ served as controls. As shown in Fig. 3*B*, protein expression of constructs was similar and LT$^{\Delta 69–83}$ did not coprecipitate detectable amounts of CUL7. Wild-type SV40 LT coprecipitated CUL7 full-length (1–1698) and CUL7 mutants spanning residues 493–1698, 779–992, or 1217–1505 with comparable efficiency. In contrast, SV40 LT failed to bind the CUL7$^{1–1390}$ mutant (Fig. 3*B*, lane 6). Taken together, these data indicate that residues 1391–1698 in the C terminus of CUL7 are critical for SV40 LT binding.

SV40 LT Enhances Activation of IRS1 Downstream Signaling Pathways. IRS1 is a central component of the insulin and IGF1 signaling pathway to transduce receptor activation to the downstream signaling pathways PI3K/AKT and Erk MAPK (18). CRL7 was shown to be part of a negative feedback loop via mTORC1/ribosomal protein S6 kinase (S6K) that restrains IRS1 signaling (17, 19). To evaluate the effect of SV40 LT on signaling pathways downstream of IRS1, full-length SV40 LT or LT$^{\Delta 69–83}$ was ectopically expressed in U2-OS cells and the activation status of AKT and Erk MAPK was analyzed by immunoblot analyses. In agreement with previous results (22), the presence of SV40 LT was associated with higher levels of activated AKT (AKT^{pS473}) (Fig. 4*A*, center lane vs. left lane). In addition, compared with control cells, significant activation of the Erk1/2 MAPK pathway (Erk$^{pT202/pY204}$) was observed. Importantly, no effect on IRS1 downstream signaling (neither AKT nor Erk MAPK) was seen upon expression of the CUL7 binding-deficient mutant LT$^{\Delta 69–83}$ (Fig. 4*A*, right lane vs. left lane). Similar results were obtained with a stable U2-OS–based cell line constitutively expressing SV40 LT or LT$^{\Delta 69–83}$ (Fig. 4*D*) or upon transient LT and LT$^{\Delta 69–83}$ transfection in HEK293 cells (Fig. S5).

Given our hypothesis that SV40 LT exerts an inhibitory effect on CUL7 function that neutralizes CRL7-mediated negative feedback control of AKT and Erk MAPK signaling, we reasoned that depletion of CUL7 should exert similar effects as SV40 LT on cell signaling. To test this hypothesis, cells (U2-OS) were transfected with siRNA directed against CUL7 mRNA and immunoblot analyses were performed after 48 h. Knockdown efficiency was ~80% (Fig. 4*B*). As shown in Fig. 4*B*, CUL7 depletion significantly enhanced phosphorylation of both AKT (AKT^{pS473}) and Erk1/2 (Erk$^{pT202/pY204}$). Similar results were also observed in C2C12 cells (23). Thus, the data obtained from the SV40 LT expression and CUL7 depletion experiments support the hypothesis that binding of SV40 LT to CUL7 impairs CRL7's function to restrain AKT and Erk MAPK signaling. To further support this model, we investigated gene expression levels of *c-fos*, a downstream target of Erk MAPK signaling (24), by quantitative real-time PCR (Fig. 4*C*). U2-OS cells transfected with siRNA directed against CUL7 displayed a 9.3-fold up-regulation of *c-fos* compared with scramble controls ($P < 0.01$). In addition, ectopic expression of LT resulted in a 10.4-fold up-regulation of *c-fos* compared with empty vector-transfected control cells ($P < 0.001$). Of note, no significant changes of *c-fos* gene expression were observed upon expression of the CUL7 binding-deficient mutant LT$^{\Delta 69–83}$.

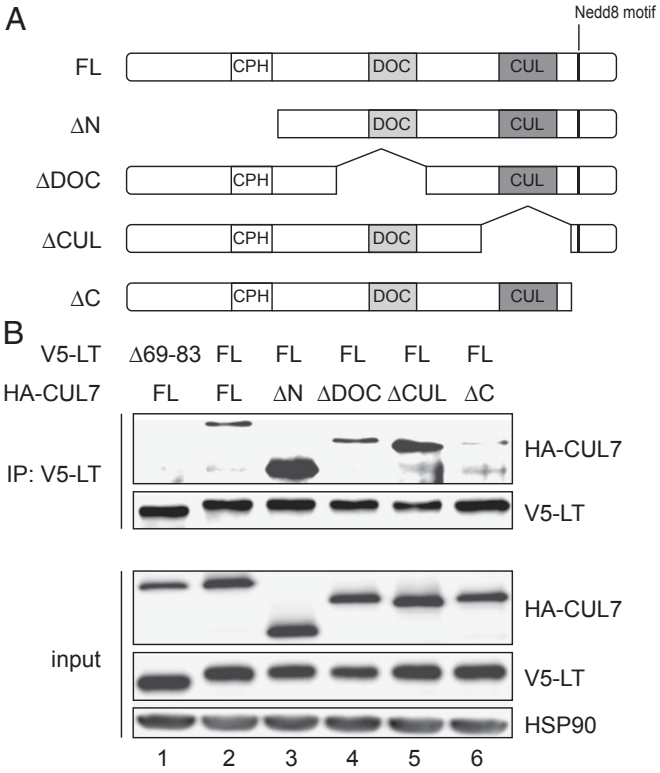

Fig. 3. SV40 LT binds to the C terminus of CUL7. (*A*) Domain map of full-length (FL) CUL7 protein and deletion mutant proteins of CUL7. (*B*) Coimmunoprecipitation of HEK293 cells transfected with V5-tagged LT or LT$^{\Delta 69–83}$ and HA-tagged CUL7 full-length or deletion mutants. Cell lysates were immunoprecipitated with V5 antibody, and precipitates were subjected to SDS/PAGE and Western blot analysis using antibodies directed against HA or V5 (*Upper*). Expression level of ectopically expressed HA- and V5-tagged proteins (*Lower*). Representative Western blot of four independent experiments.

BIOCHEMISTRY

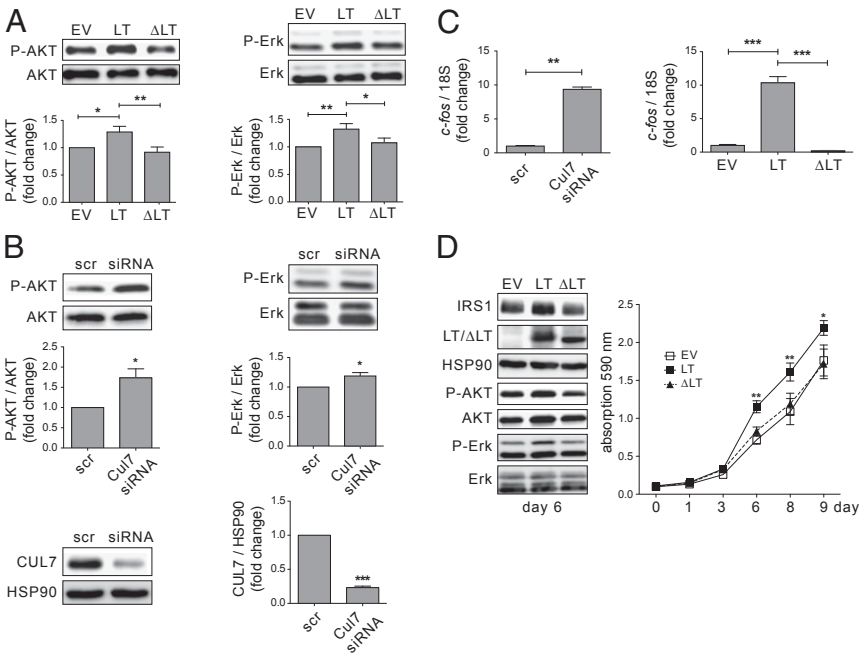

Fig. 4. Activation of AKT and Erk MAPK signaling upon LT expression or CUL7 siRNA depletion. Lysates were subjected to SDS/PAGE and Western blot analysis using antibodies directed against AKT^{pS473}, Erk$^{pT202/pY204}$, AKT, and Erk. (*A*) U2-OS cells were transfected with empty vector (EV) or plasmids encoding HA-tagged LT or LT$^{\Delta 69-83}$. $n = 10$; $^{*}P < 0.05$, $^{**}P < 0.01$. (*B*) U2-OS cells were transfected with scramble (scr) siRNA or siRNA directed against CUL7 mRNA. $n = 4$–5; $^{*}P < 0.05$, $^{***}P < 0.001$. (*C*) The Erk MAPK downstream target gene *c-fos* is up-regulated upon siRNA-mediated CUL7 depletion or ectopic expression of LT but not ΔLT. U2-OS cells were transfected as described in *A* and *B*. Total mRNA was isolated, reverse-transcribed to cDNA, and analyzed for *c-fos* by quantitative real-time PCR. $n = 3$; $^{**}P < 0.01$, $^{***}P < 0.001$. (*D*) U2-OS cells were infected with retroviruses containing pBABE EV, LT, or LT$^{\Delta 69-83}$. (*Left*) Representative blot of whole-cell lysates at day 6. (*Right*) Proliferation assay of U2-OS cells stably expressing EV (white boxes), LT (black boxes), or ΔLT (black triangles). Each data point represents an average of eight samples. Cell density was assayed by crystal violet staining and is expressed as photometric absorption at 590 nm. $^{*}P < 0.05$, $^{**}P < 0.01$. Data are presented as means ± SEM.

SV40 LT-Positive Carcinoma Displays Higher IRS1 Protein Levels and Enhanced IRS1-Dependent Signaling in Vivo. To assess the relevance of SV40 LT-triggered deregulation of IRS1 protein and signaling pathways in vivo, we examined tumor tissue derived from carcinoembryonic antigen (CEA)424/SV40 LT transgenic mice, an established animal model of early-onset invasive gastric carcinoma (25). Expression of SV40 LT under the control of the gut-specific 424-bp CEA promoter resulted in the development of multifocal carcinomas in the pyloric region of the stomach in all offspring (25). Histopathological analysis of gastrointestinal tissue of 90-d-old mice was performed by immunofluorescence microscopy and the signal intensity was quantified using ImageJ (National Institutes of Health). In keeping with previous reports (26), CEA promoter-driven SV40 LT expression was associated with substantial malignant transformation of the pyloric and duodenal mucosal layer with formation of neuroendocrine carcinomas (Fig. 5). In these samples, expression of SV40 LT in tumorous tissue was correlated positively with both elevated IRS1 protein level ($R = 0.529$, $P = 0.0241$) and activation of the downstream signaling pathway Erk MAPK (Erk$^{pT202/pY204}$; $R = 0.629$, $P = 0.0051$) (Fig. 5 *A* and *C*). Compared with untransformed LT-negative tissue, transgenic expression of SV40 LT led to an approximately twofold increase in IRS1 protein concentration and phosphorylation of Erk$^{pT202/pY204}$ (Fig. 5 *A* and *B*). Of note, retroviral expression of IRS1 was associated with enhanced PI3K/AKT and Erk MAPK signaling in IMR90 fibroblasts (Fig. S6), thus underscoring the potential of accumulated IRS1 proteins to promote the activation of downstream pathways. Interestingly, IRS1 accumulation was not homogeneous among SV40 LT-expressing cells and was most prevalent in SV40 LT-positive cells infiltrating the lamina mucosae (Fig. 5*A*). Thus, the in vivo findings are in accordance with the data obtained from the cell-based and in vitro experiments and strongly suggest that SV40 LT inhibits CRL7 function, which results in deregulated IRS1 signaling.

Discussion

SV40 LT is a powerful viral oncoprotein with the ability to transform cells and promote oncogenesis (1, 2). The transforming activity of SV40 LT has been attributed to its ability to bind and inactivate tumor suppressor proteins p53 and members of the pRB family. However, genetic studies revealed that its association with other host cell factors was required for full transformation and oncogenesis (27). Of these, CUL7, a core component of CRL7, was shown to be required for SV40 LT transformation independent of p53/pRB inactivation or viral replication (9).

In this work, we provide compelling evidence that binding of SV40 LT to CUL7 impairs the ability of CRL7 to mediate ubiquitin-dependent degradation of IRS1, thereby leading to deregulation of IRS1 downstream signaling pathways AKT and Erk MAPK. We showed that (*i*) SV40 LT binds to the C-terminal domain of CUL7 spanning residues 1391–1698, (*ii*) expression of SV40 LT, but not of CUL7 binding-deficient mutant LT$^{\Delta 69-83}$, results in prolonged protein half-life and cellular accumulation of IRS1, (*iii*) SV40 LT inhibits CRL7-mediated polyubiquitination of IRS1 in vitro, and (*iv*) SV40 LT expression or CUL7 depletion results in hyperactivation of IRS1 downstream signaling pathways AKT and Erk MAPK and up-regulation of the downstream target gene *c-fos*. Finally, SV40 LT-positive carcinomas of transgenic CEA424/SV40 LT mice exhibited markedly increased IRS1 protein and phosphorylated Erk1/2 (Erk$^{pT202/pY204}$) levels compared with nontransformed tissue. These findings led us to hypothesize that SV40 LT acts to neutralize CRL7 activity, which might contribute to SV40-induced oncogenesis. In this model, the inhibition of CRL7-mediated proteasomal degradation of IRS1 by SV40 LT causes sustained promitogenic AKT and Erk MAPK signaling (Fig. S7).

DeCaprio and coworkers mapped the CUL7 interaction domain on LT to an exposed loop spanning residues 69–83 in the N terminus of SV40 LT, a site distinct from the binding domains for p53 or pRB members (9). Moreover, the authors showed that all CRL7 components coimmunoprecipitate with SV40 LT, indicating that SV40 LT does not disrupt CRL7 complex formation. In this study, we mapped the SV40 LT interaction domain on CUL7 to the C-terminal residues 1391–1698. The C terminus of cullin proteins harbors the conserved cullin homology domain for binding of RING partner ROC1 or ROC2 that recruits the ubiquitin-loaded E2 enzymes for catalysis (21). Based on structural work on the CUL1–ROC1 association (28), CUL7's C terminus is projected to form multiple interface interactions with the N-terminal S1 β-strand of ROC1. In addition, the C terminus of most, if not all, cullins is covalently conjugated with the

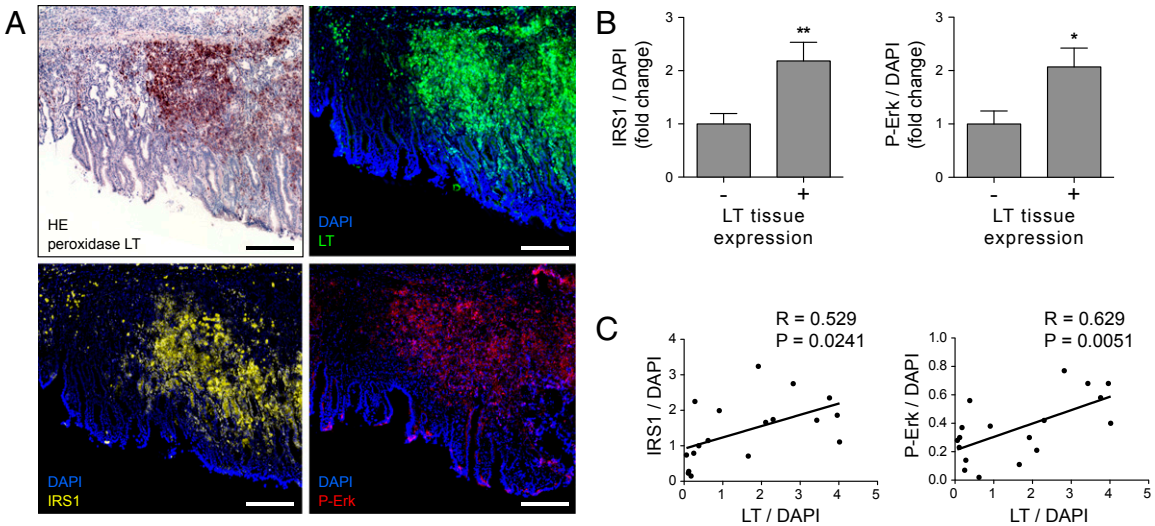

Fig. 5. Increased IRS1 protein level and signaling in carcinomas of CEA424/SV40 LT mice. (*A*) Peroxidase/HE staining (*Left Upper*) or immunofluorescence for LT (green), IRS1 (yellow), Erk$^{pT202/pY204}$ (red), and nuclear costaining with DAPI (blue) of pyloric tissue in 90-d-old CEA424/SV40 LT mice. (Scale bars, 100 μm.) (*B*) Quantification of the mean intensities of IRS1 (*Left*) and Erk$^{pT202/pY204}$ (*Right*) in LT-positive vs. -negative tissue. Eighteen randomly selected areas of four different tissue samples were quantified using ImageJ software and normalized to DAPI intensities. $*P < 0.05$, $**P < 0.01$. Data are presented as means ± SEM. (*C*) Regression analysis of LT expression with IRS1 (*Left*) or Erk$^{pT202/pY204}$ staining intensities (*Right*).

ubiquitin-like molecule NEDD8. Modification with NEDD8, termed neddylation, activates E3 ligase activity of CRLs by promoting substrate polyubiquitination (29). In vitro mutagenesis experiments and structural studies have suggested that conjugation of NEDD8 to CUL1 induces conformational changes required for ubiquitin transfer, thereby driving CRLs into an active state (30, 31). It remains to be determined whether SV40 LT impairs CRL7 function through disrupting activities associated with the C terminus of CUL7 in supporting the ROC1 RING and/or neddylation.

At a cellular level, IRS1 and its downstream signaling pathways have been directly linked to cellular transformation by SV40 LT. IRS proteins do not contain intrinsic kinase activity but rather function by organizing signaling complexes to initiate intracellular signaling cascades (18). It has been shown that signaling through the IGF1 receptor is essential for transformation by SV40 LT (7, 32, 33). Cells that do not express IRS1 or that contain inactive IRS1 species failed to be transformed in culture in the presence of LT, which could be overcome by expression of a constitutively active p110 subunit of PI3K (a target of IRS1) (33). Yu and Alwine (22, 34) reported that expression of SV40 LT activates AKT, which could be prevented by the PI3K inhibitor LY294002, suggesting that SV40 LT interferes with the signaling cascade upstream of PI3K. Our observation that SV40 LT, but not the CUL7 binding-deficient mutant LT$^{\Delta 69-83}$, activates AKT and Erk MAPK pathways suggests that viral transformation may require suppression of CRL7-mediated degradation of IRS1. It should be noted that despite repeated efforts, we have been unable to observe accumulation of endogenous IRS1 protein upon transient expression of SV40 LT on a constant basis using immunoblot analysis. On the other hand, in CEA424/SV40 LT mice, SV40 LT expression was reproducibly associated with elevated levels of endogenous IRS1 protein as shown by immunofluorescence imaging experiments (Fig. 5). In addition, CUL7 silencing by siRNA was shown to prevent insulin-induced degradation of IRS1 in C2C12 myotubes (23), thus further underscoring the requirement of CUL7 for the control of IRS1 homeostasis. These differences might be due to the complexity of multiple E3 ligases controlling IRS1 stability (35–37). It is possible that SV40 LT only impacts a subset of IRS1 that directly participates in PI3K/Erk MAPK signaling. Despite this uncertainty, multiple in vivo and in vitro results, as summarized above, suggest a role for SV40 LT in protecting IRS1 from CRL7-mediated degradation.

We previously reported that CRL7-mediated turnover of IRS1 is dependent on mTORC1/S6K1 signaling (17). In addition, IRS1 protein homeostasis was shown to be regulated by mTORC2-mediated stabilization of Fbw8 (20) and liver kinase B1-controlled Fbw8 gene expression (38). Our observation that SV40 LT-positive carcinomas of CEA424/SV40 LT mice exhibited twofold increased IRS1 levels and Erk MAPK activation compared with normal tissue suggests that SV40 LT acts to disrupt CRL7-mediated feedback control of IRS1. Interestingly, the viral early region of SV40 encodes the small T antigen (ST) that supports LT in cell transformation. SV40 ST inactivates serine-threonine protein phosphatase A, thereby leading to increased AKT signaling via activation of PI3K (39, 40). It is thus tempting to speculate that SV40 LT and ST cooperate to perturb IRS1 signaling using distinct mechanisms for cellular transformation.

Numerous studies have established a causal link between aberrant activation of PI3K/AKT and Erk MAPK signaling and tumorigenesis (41). A role for a negative feedback loop via IRS1 in controlling cancer was first revealed in a study with mice heterozygous for tuberous sclerosis 2 (*Tsc2*) (42). TSC2 is an inhibitor of small GTPase RHEB and hence the loss of TSC2 leads to activation of mTOR/S6K. It was shown that *Tsc2*$^{+/-}$ mice develop benign hemangiomas due to sporadic loss of the functional *Tsc2* allele. The lack of malignant tumor development results from inactive AKT, because highly activated mTOR/S6K triggers an IRS1-mediated negative feedback loop to suppress PI3K. In keeping with this concept, circumventing the IRS1 negative feedback loop by reduction of PTEN activity resulted in enhanced AKT activation, as well as more frequent and aggressive hemangiomas (42).

Together with these findings, the data described here point to a model in which SV40 LT increases IRS1 downstream signaling by suppressing the CRL7-mediated negative feedback loop (Fig. S7). We propose that the perturbation of CRL7-controlled promitogenic signaling as reported above constitutes a previously unrecognized pathogenic mechanism of SV40 transformation and oncogenesis. Of note, a previous study by Lee and coworkers demonstrated that mice with transgenic expression of IRS1 in the mammary gland develop progressive mammary hyperplasia,

tumorigenesis, and metastasis (43), thus further supporting the oncogenic potential of IRS1 that may be exploited by SV40. Our attempts to directly address the role of IRS1 in SV40 transformation have been hampered by technical difficulties resulting from cell toxicity. Further studies are thus needed to develop suitable cell-transformation systems to precisely delineate the molecular interplay and biological role of SV40 LT with CRL7-regulated IRS1 protein homeostasis and signaling of the host cell.

Materials and Methods

^{35}S Pulse–Chase Labeling. At 24 h posttransfection, cells (HEK293) were incubated with methionine/cysteine-free DMEM (PAN-Biotech) supplemented with 10 mM Hepes (pH 7.4), 1% L-glutamine, and 1% penicillin/streptomycin (all PAN-Biotech) for 45 min at 37 °C and 5% (vol/vol) CO_2, followed by pulsing with 50 μCi/mL [^{35}S]methionine/cysteine for 60 min. After labeling, cells were chased in normal DMEM growth medium for the time periods indicated. Lysates were subjected to V5 immunoprecipitation (IP) and SDS/PAGE, and radioactivity was quantitated by autoradiography using a Cyclone Plus Phosphor Imager (PerkinElmer).

In Vitro Ubiquitination. GST-IRS1$^{1–574}$ was expressed in a baculovirus/High Five insect cell system and purified as described (19). Reaction mixtures (20 μL) containing 1.1 pmol GST-IRS1$^{1–574}$, 50 mM Tris·HCl (pH 7.4), 5 mM $MgCl_2$, 0.5 mM DTT, 2 mM ATP, 2 mM NaF, 10 nM okadaic acid, 0.2 pmol CRL7, 50 μM PK-Ub, 13 nM E1, and 1 μM UbcH5c were incubated at 37 °C, and increasing amounts of LT protein (0.5–9.0 pmol) were added (for isolation of SV40 LT, see ref. 44). Reaction products were separated by 4–20% SDS/PAGE and analyzed by anti-GST (Santa Cruz Biotechnology) immunoblot analysis.

Microscopy. Animal studies within this work were registered and accredited by the local regulatory agency (Regierung von Oberbayern, Munich) with registration number Z02. For immunofluorescence microscopy, cryosections were fixed in acetone and blocked in 10% (vol/vol) goat serum. After incubation with primary antibodies directed against IRS1 (06-248; Millipore), SV40 T antigen (v-300, sc-20800; Santa Cruz Biotechnology), or P-Erk (pT202/pY204, 9101; Cell Signaling) and secondary antibody Alexa Fluor 594 (Invitrogen), slides were mounted with DAPI (Vector Laboratories). Peroxidase and hematoxylin/eosin (HE) staining were performed as described previously (26). An Axio Observer Z1 microscope (Zeiss) was used for analysis.

Statistics. Data are presented as means ± SEM. To test the statistical difference between means of two (*t* test) or more groups (ANOVA), linear regression analysis GraphPad Prism 5.0 software was used. *P* values <0.05 were considered significant.

ACKNOWLEDGMENTS. We thank Claus Schwechheimer for critical discussion of the manuscript, and Azad Bonni and James DeCaprio (Harvard Medical School) and Jim Manfredi (Mount Sinai School of Medicine) for generously providing plasmids. This work was supported by Research Grant SA 1706/3-1 from the German Research Foundation (to A.S.) and Marie Curie International Reintegration Grant 256584 (to A.S.). Z.-Q.P. was supported by U.S. Public Health Service Grants GM61051 and CA095634.

1. Cheng J, DeCaprio JA, Fluck MM, Schaffhausen BS (2009) Cellular transformation by simian virus 40 and murine polyoma virus T antigens. *Semin Cancer Biol* 19(4): 218–228.
2. Sullivan CS, Pipas JM (2002) T antigens of simian virus 40: Molecular chaperones for viral replication and tumorigenesis. *Microbiol Mol Biol Rev* 66(2):179–202.
3. DeCaprio JA (2009) How the Rb tumor suppressor structure and function was revealed by the study of Adenovirus and SV40. *Virology* 384(2):274–284.
4. Kohrman DC, Imperiale MJ (1992) Simian virus 40 large T antigen stably complexes with a 185-kilodalton host protein. *J Virol* 66(3):1752–1760.
5. Daud AI, Lanson NA, Jr., Claycomb WC, Field LJ (1993) Identification of SV40 large T-antigen-associated proteins in cardiomyocytes from transgenic mice. *Am J Physiol* 264(5 Pt 2):H1693–H1700.
6. Fei ZL, D'Ambrosio C, Li S, Surmacz E, Baserga R (1995) Association of insulin receptor substrate 1 with simian virus 40 large T antigen. *Mol Cell Biol* 15(8):4232–4239.
7. Sell C, et al. (1993) Simian virus 40 large tumor antigen is unable to transform mouse embryonic fibroblasts lacking type 1 insulin-like growth factor receptor. *Proc Natl Acad Sci USA* 90(23):11217–11221.
8. Ali SH, Kasper JS, Arai T, DeCaprio JA (2004) Cul7/p185/p193 binding to simian virus 40 large T antigen has a role in cellular transformation. *J Virol* 78(6):2749–2757.
9. Kasper JS, Kuwabara H, Arai T, Ali SH, DeCaprio JA (2005) Simian virus 40 large T antigen's association with the CUL7 SCF complex contributes to cellular transformation. *J Virol* 79(18):11685–11692.
10. Dias DC, Dolios G, Wang R, Pan Z-Q (2002) CUL7: A DOC domain-containing cullin selectively binds Skp1.Fbx29 to form an SCF-like complex. *Proc Natl Acad Sci USA* 99(26):16601–16606.
11. Sarikas A, Xu X, Field LJ, Pan Z-Q (2008) The cullin7 E3 ubiquitin ligase: A novel player in growth control. *Cell Cycle* 7(20):3154–3161.
12. Arai T, et al. (2003) Targeted disruption of p185/Cul7 gene results in abnormal vascular morphogenesis. *Proc Natl Acad Sci USA* 100(17):9855–9860.
13. Tsunematsu R, et al. (2006) Fbxw8 is essential for Cul1-Cul7 complex formation and for placental development. *Mol Cell Biol* 26(16):6157–6169.
14. Huber C, et al. (2005) Identification of mutations in CUL7 in 3-M syndrome. *Nat Genet* 37(10):1119–1124.
15. Huber C, et al. (2009) A large-scale mutation search reveals genetic heterogeneity in 3M syndrome. *Eur J Hum Genet* 17(3):395–400.
16. Maksimova N, et al. (2007) Clinical, molecular and histopathological features of short stature syndrome with novel CUL7 mutation in Yakuts: New population isolate in Asia. *J Med Genet* 44(12):772–778.
17. Xu X, et al. (2008) The CUL7 E3 ubiquitin ligase targets insulin receptor substrate 1 for ubiquitin-dependent degradation. *Mol Cell* 30(4):403–414.
18. White MF (2002) IRS proteins and the common path to diabetes. *Am J Physiol Endocrinol Metab* 283(3):E413–E422.
19. Xu X, et al. (2012) Identification of the degradation determinants of insulin receptor substrate 1 for signaling cullin-RING E3 ubiquitin ligase 7-mediated ubiquitination. *J Biol Chem* 287(48):40758–40766.
20. Kim SJ, et al. (2012) mTOR complex 2 regulates proper turnover of insulin receptor substrate-1 via the ubiquitin ligase subunit Fbw8. *Mol Cell* 48(6):875–887.
21. Sarikas A, Hartmann T, Pan Z-Q (2011) The cullin protein family. *Genome Biol* 12(4):220.
22. Yu Y, Alwine JC (2008) Interaction between simian virus 40 large T antigen and insulin receptor substrate 1 is disrupted by the K1 mutation, resulting in the loss of large T antigen-mediated phosphorylation of Akt. *J Virol* 82(9):4521–4526.
23. Scheufele F, et al. (2014) Evidence for a regulatory role of Cullin-RING E3 ubiquitin ligase 7 in insulin signaling. *Cell Signal* 26(2):233–239.
24. Roskoski R, Jr. (2012) ERK1/2 MAP kinases: Structure, function, and regulation. *Pharmacol Res* 66(2):105–143.
25. Thompson J, et al. (2000) A transgenic mouse line that develops early-onset invasive gastric carcinoma provides a model for carcinoembryonic antigen-targeted tumor therapy. *Int J Cancer* 86(6):863–869.
26. Ihler F, et al. (2012) Expression of a neuroendocrine gene signature in gastric tumor cells from CEA 424-SV40 large T antigen-transgenic mice depends on SV40 large T antigen. *PLoS ONE* 7(1):e29846.
27. Sachsenmeier KF, Pipas JM (2001) Inhibition of Rb and p53 is insufficient for SV40 T-antigen transformation. *Virology* 283(1):40–48.
28. Zheng N, et al. (2002) Structure of the Cul1-Rbx1-Skp1-F box^{Skp2} SCF ubiquitin ligase complex. *Nature* 416(6882):703–709.
29. Pan ZQ, Kentsis A, Dias DC, Yamoah K, Wu K (2004) Nedd8 on cullin: Building an expressway to protein destruction. *Oncogene* 23(11):1985–1997.
30. Yamoah K, et al. (2008) Autoinhibitory regulation of SCF-mediated ubiquitination by human cullin 1's C-terminal tail. *Proc Natl Acad Sci USA* 105(34):12230–12235.
31. Duda DM, et al. (2008) Structural insights into NEDD8 activation of cullin-RING ligases: Conformational control of conjugation. *Cell* 134(6):995–1006.
32. Porcu P, et al. (1992) The growth-stimulatory effect of simian virus 40 T antigen requires the interaction of insulinlike growth factor 1 with its receptor. *Mol Cell Biol* 12(11):5069–5077.
33. DeAngelis T, Chen J, Wu A, Prisco M, Baserga R (2006) Transformation by the simian virus 40 T antigen is regulated by IGF-I receptor and IRS-1 signaling. *Oncogene* 25(1):32–42.
34. Yu Y, Alwine JC (2002) Human cytomegalovirus major immediate-early proteins and simian virus 40 large T antigen can inhibit apoptosis through activation of the phosphatidylinositide 3′-OH kinase pathway and the cellular kinase Akt. *J Virol* 76(8): 3731–3738.
35. Rui L, Yuan M, Frantz D, Shoelson S, White MF (2002) SOCS-1 and SOCS-3 block insulin signaling by ubiquitin-mediated degradation of IRS1 and IRS2. *J Biol Chem* 277(44): 42394–42398.
36. Nakao R, et al. (2009) Ubiquitin ligase Cbl-b is a negative regulator for insulin-like growth factor 1 signaling during muscle atrophy caused by unloading. *Mol Cell Biol* 29(17):4798–4811.
37. Shi J, Luo L, Eash J, Ibebunjo C, Glass DJ (2011) The SCF-Fbxo40 complex induces IRS1 ubiquitination in skeletal muscle, limiting IGF1 signaling. *Dev Cell* 21(5):835–847.
38. Zhang W, Wang Q, Song P, Zou M-H (2013) Liver kinase b1 is required for white adipose tissue growth and differentiation. *Diabetes* 62(7):2347–2358.
39. Pallas DC, et al. (1990) Polyoma small and middle T antigens and SV40 small t antigen form stable complexes with protein phosphatase 2A. *Cell* 60(1):167–176.
40. Yuan H, Veldman T, Rundell K, Schlegel R (2002) Simian virus 40 small tumor antigen activates AKT and telomerase and induces anchorage-independent growth of human epithelial cells. *J Virol* 76(21):10685–10691.
41. Vivanco I, Sawyers CL (2002) The phosphatidylinositol 3-kinase AKT pathway in human cancer. *Nat Rev Cancer* 2(7):489–501.
42. Manning BD, et al. (2005) Feedback inhibition of Akt signaling limits the growth of tumors lacking Tsc2. *Genes Dev* 19(15):1773–1778.
43. Dearth RK, et al. (2006) Mammary tumorigenesis and metastasis caused by overexpression of insulin receptor substrate 1 (IRS-1) or IRS-2. *Mol Cell Biol* 26(24):9302–9314.
44. Mastrangelo IA, et al. (1989) ATP-dependent assembly of double hexamers of SV40 T antigen at the viral origin of DNA replication. *Nature* 338(6217):658–662.